

# Effective quantum dynamics on the Möbius strip

Tomáš Kalvoda,<sup>a</sup> David Krejčířík<sup>b</sup> and Kateřina Zahradová<sup>c</sup>

a) *Department of Applied Mathematics, Faculty of Information Technology, Czech Technical University in Prague, Thákurova 9, 16000 Prague 6, Czechia; tomas.kalvoda@fit.cvut.cz.*

b) *Department of Mathematics, Faculty of Nuclear Sciences and Physical Engineering, Czech Technical University in Prague, Trojanova 13, 12000 Prague 2, Czechia; david.krejcirik@fjfi.cvut.cz.*

c) *School of Mathematical Sciences, Queen Mary University of London, London E 4NS, United Kingdom; k.zahradova@qmul.ac.uk.*

September 8, 2021

## Abstract

The Laplace–Beltrami operator in the curved Möbius strip is investigated in the limit when the width of the strip tends to zero. By establishing a norm-resolvent convergence, it is shown that spectral properties of the operator are approximated well by an unconventional flat model whose spectrum can be computed explicitly in terms of Mathieu functions. Contrary to the traditional flat Möbius strip, our effective model contains a geometric potential. A comparison of the three models is made and analytical results are accompanied by numerical computations.

**Keywords:** Mbius strip, Laplace–Beltrami operator, spectrum, effective Hamiltonian, resolvent convergence, quantisation on submanifolds.

## 1 Introduction

The unorientable nature of the Möbius strip has fascinated scientists as well as laypeople since its discovery in the nineteenth century (see [14] for a popular overview), or perhaps even before (*cf.* [6]). In this paper we are interested in the interplay between the peculiar geometry of the Möbius strip and its physical properties quantified by spectral data, which seems to have escaped the attention of the scientific community so far.

**The true model.** We start with the traditional geometric realisation of the Möbius strip as a two-dimensional ruled surface built along a circle of radius  $R > 0$  in  $\mathbb{R}^3$ :

$$\Omega := \left\{ \left( \left[ R - t \cos \left( \frac{s}{2R} \right) \right] \cos \left( \frac{s}{R} \right), \left[ R - t \cos \left( \frac{s}{2R} \right) \right] \sin \left( \frac{s}{R} \right), -t \sin \left( \frac{s}{2R} \right) \right) : s \in [0, 2\pi R), t \in (-a, a) \right\}, \quad (1)$$

where  $a \in (0, R)$  is the half-width of the strip, see Figure 1. Notice that the surface  $\Omega$  is not orientable due to the division of the angle  $s/R$  by the factor two, while the strip is still well “glued together” at the endpoints corresponding to  $s = 0$  and  $s = 2\pi R$ . We consider the self-adjoint operator

$$-\Delta_D^\Omega \quad \text{in} \quad L^2(\Omega),$$

which acts as Laplace–Beltrami operator in  $\Omega$  and satisfies Dirichlet boundary conditions on  $\partial\Omega$ . Depending on whether we consider the wave, heat or Schrödinger equation on  $\Omega$ , the eigenvalues and eigenfunctions of  $-\Delta_D^\Omega$  have various physical meaning. Here we mostly use the quantum-mechanical language, where  $-\Delta_D^\Omega$  is the Hamiltonian of an electron constrained to  $\Omega$  by hard-wall boundaries and the eigenvalues and eigenfunctions correspond to bound-state energies and wave-functions, respectively. (In order to simultaneously consider the other physical models, we disregard the possibility of adding a geometric potential due to the embedding of  $\Omega$  in  $\mathbb{R}^3$ , see [11] and references therein.) When interested in analytic properties of the Möbius strip  $\Omega$ , we call  $-\Delta_D^\Omega$  the *true* (or *full*) model.

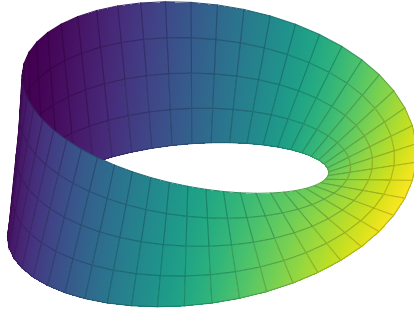


Figure 1: Möbius strip  $\Omega$  built along a circle of radius  $R$  and with width  $2a$ , see (1).

**The fake model.** The weak point of the true model  $-\Delta_D^\Omega$  is that its spectrum cannot be computed explicitly (for numerical calculations, see, *e.g.*, [13, 12], and below). On the other hand, the spectrum of the *flat* model  $-\Delta_D^{\Omega_0}$  represented by the Laplacian in

$$\Omega_0 := (0, 2\pi R) \times (-a, a),$$

subject to Dirichlet boundary conditions

$$\psi(s, \pm a) = 0 \tag{2}$$

for almost every  $s \in (0, 2\pi R)$  and twisted periodic boundary conditions

$$\psi(0, t) = \psi(2\pi R, -t), \tag{3}$$

$$\partial_1 \psi(0, t) = \partial_1 \psi(2\pi R, -t), \tag{4}$$

for almost every  $t \in (-a, a)$ , is explicitly computable. Indeed, by considering the spectral problem (which can be solved by separation of variables) for the Laplacian in the extended strip  $(-2\pi R, 2\pi R) \times (-a, a)$ , subject to Dirichlet boundary conditions on  $(0, 2\pi R) \times \{\pm a\}$  and standard periodic boundary conditions on  $\{\pm 2\pi R\} \times (-a, a)$ , by symmetry arguments one easily arrives at

$$\sigma(-\Delta_D^{\Omega_0}) = \left\{ \left( \frac{m}{2R} \right)^2 + \left( \frac{n\pi}{2a} \right)^2 \right\}_{\substack{m \in \mathbb{Z} \\ n \in \mathbb{N}^* \\ m+n \text{ odd}}}, \tag{5}$$

where  $\mathbb{N}^* := \mathbb{N} \setminus \{0\}$  (the set  $\mathbb{N}$  of all natural numbers contain zero in our convention). At the same time, the eigenfunctions corresponding to the eigenvalues in (5) are explicit combinations of sines and cosines. While the flat model  $-\Delta_D^{\Omega_0}$  keeps the topology of the Möbius strip, it completely disregards the curved nature of  $\Omega$ , and for this reason we also call it the *fake* model. Of course, there is no reason to expect that the spectrum (5) is in any sense related to (*i.e.*, approximating) the spectrum of  $-\Delta_D^\Omega$ .

**The not-so-fake model.** The main objective of this paper is to introduce a new model of the Möbius strip, whose spectrum is explicitly computable and simultaneously approximates the spectrum of the true model  $-\Delta_D^\Omega$  in the limit of *thin* strips, *i.e.*  $a \rightarrow 0$ . This *not-so-fake* (or *effective*) model is given by the perturbed operator

$$H_{\text{eff}} := -\Delta_D^{\Omega_0} + V_{\text{eff}} \quad \text{with} \quad V_{\text{eff}}(s, t) := -\frac{1}{8R^2} \cos\left(\frac{s}{R}\right). \tag{6}$$

Hence, the addition of the geometric potential  $V_{\text{eff}}$  to the fake model is necessary to get a more realistic approximation of the dynamics. In accordance with general thin strips [10, Sec. 3], we have  $V_{\text{eff}}(s, t) = -\frac{1}{4}\kappa_g(s)^2 - \frac{1}{2}K(s, 0)$ , where  $K$  is the Gauss curvature of  $\Omega$  and  $\kappa_g$  is the geodesic curvature of the underlying circle as a curve on the surface  $\Omega$ , see Remark 3. The aforementioned approximation in thin

strips will be justified by showing that the norm of the difference of the resolvents of  $-\Delta_D^\Omega$  and  $H_{\text{eff}}$  vanishes as  $a \rightarrow 0$ . Two remarks are in order. First, since the operators act in different Hilbert spaces, a natural identification is necessary. Second, since the eigenvalues tend to infinity as  $a \rightarrow 0$ , see (8) below, it does not really make sense to compare the resolvents  $(-\Delta_D^\Omega - z)^{-1}$  and  $(H_{\text{eff}} - z)^{-1}$  (at least with an  $a$ -independent  $z$ ); instead we consider renormalised operators by subtracting the lowest transverse energy

$$E_1 := \left(\frac{\pi}{2a}\right)^2.$$

Namely, we prove (see Theorem 1)

$$\|U(-\Delta_D^\Omega - E_1 - z)^{-1}U^{-1} - (H_{\text{eff}} - E_1 - z)^{-1}\| = O(a) \quad \text{as } a \rightarrow 0, \quad (7)$$

where  $U : L^2(\Omega) \rightarrow L^2(\Omega_0)$  is a suitable unitary transform and  $z$  is any  $a$ -independent number lying simultaneously in the resolvent sets of the shifted operators  $-\Delta_D^\Omega - E_1$  and  $H_{\text{eff}} - E_1$ . In other words, we establish the norm-resolvent convergence in a generalised sense. An advantage of this approximation is that (by the same extension trick as for the fake model above) the spectrum of  $H_{\text{eff}}$  can be computed explicitly:

$$\sigma(H_{\text{eff}}) = \left\{ \left(\frac{1}{2R}\right)^2 a_m \left(-\frac{1}{4}\right) + \left(\frac{n\pi}{2a}\right)^2 \right\}_{\substack{m \in \mathbb{N} \\ n \in \mathbb{N}^* \\ m+n \text{ odd}}} \cup \left\{ \left(\frac{1}{2R}\right)^2 b_m \left(-\frac{1}{4}\right) + \left(\frac{n\pi}{2a}\right)^2 \right\}_{\substack{m \in \mathbb{N}^* \\ n \in \mathbb{N}^* \\ m+n \text{ odd}}}, \quad (8)$$

where  $a_m$  and  $b_m$  are Mathieu characteristic values (see Remark 2 below and [2, Sec. 20]). The eigenfunctions corresponding to the eigenvalues in (8) are this time explicit combinations of Mathieu integral order functions.

**Organisation of the paper.** The fake and not-so-fake models are studied in Sections 2 and 3, respectively, where we particularly establish the spectral results (5) and (8) and determine the corresponding eigenfunctions. The norm-resolvent convergence (7) is established in Section 4. Our analytical results are illustrated by numerical computations in Section 5. In particular, we show the suboptimality of the rate  $O(a)$  in the approximation of the spectrum of  $-\Delta_D^\Omega$  by the spectrum of the not-so-fake model  $H_{\text{eff}}$ .

## 2 The fake model

The fake model is introduced as the operator  $-\Delta_D^{\Omega_0}$  in  $L^2(\Omega_0)$  defined by

$$\begin{aligned} -\Delta_D^{\Omega_0} \psi &:= -\Delta \psi, \\ \mathcal{D}(-\Delta_D^{\Omega_0}) &:= \{ \psi \in W^{2,2}(\Omega_0) : \psi \text{ satisfies (2) and (3)–(4)} \}, \end{aligned}$$

where the boundary conditions are understood in the sense of Sobolev-space traces (see, *e.g.*, [3]).

**Proposition 1.**  $-\Delta_D^{\Omega_0}$  is a positive self-adjoint operator with compact resolvent.

*Proof.* The operator is clearly densely defined. Let  $\|\cdot\|$  and  $(\cdot, \cdot)$  denote the norm and inner product of  $L^2(\Omega_0)$ . For every  $\psi \in \mathcal{D}(-\Delta_D^{\Omega_0})$ , we have

$$\begin{aligned} (\psi, -\Delta_D^{\Omega_0} \psi) &= \|\nabla \psi\|^2 - \int_{-a}^a \left[ \bar{\psi}(s, t) \partial_1 \psi(s, t) \right]_{s=0}^{s=2\pi R} dt - \int_0^{2\pi R} \left[ \bar{\psi}(s, t) \partial_2 \psi(s, t) \right]_{t=-a}^{t=a} ds \\ &= \|\nabla \psi\|^2, \end{aligned}$$

where the second boundary integral on the first line vanishes because of (2) and, using (3)–(4) together with an integral substitution,

$$\begin{aligned} \int_{-a}^a \left[ \bar{\psi}(s, t) \partial_1 \psi(s, t) \right]_{s=0}^{s=2\pi R} dt &= \int_{-a}^a \bar{\psi}(2\pi R, t) \partial_1 \psi(2\pi R, t) dt - \int_{-a}^a \bar{\psi}(0, t) \partial_1 \psi(0, t) dt \\ &= \int_{-a}^a \bar{\psi}(0, -t) \partial_1 \psi(0, -t) dt - \int_{-a}^a \bar{\psi}(0, t) \partial_1 \psi(0, t) dt \\ &= \int_{-a}^a \bar{\psi}(0, u) \partial_1 \psi(0, u) du - \int_{-a}^a \bar{\psi}(0, t) \partial_1 \psi(0, t) dt = 0. \end{aligned}$$

Hence,  $-\Delta_D^{\Omega_0}$  is obviously symmetric. At the same time, using the Poincaré-type inequality

$$\forall f \in W_0^{1,2}((-a, a)), \quad \int_{-a}^a |f'(t)|^2 dt \geq E_1 \int_{-a}^a |f(t)|^2 dt, \quad (9)$$

we have

$$(\psi, -\Delta_D^{\Omega_0} \psi) = \|\nabla \psi\|^2 \geq \|\partial_2 \psi\|^2 \geq E_1 \|\psi\|^2, \quad (10)$$

so  $-\Delta_D^{\Omega_0}$  is a positive operator whose spectrum does not start below  $E_1$ . To see that  $-\Delta_D^{\Omega_0}$  is self-adjoint is more subtle. A possibility how to verify it is to consider the closed quadratic form

$$\begin{aligned} Q_D^{\Omega_0}[\psi] &:= \|\nabla \psi\|^2, \\ \mathsf{D}(Q_D^{\Omega_0}) &:= \{\psi \in W^{1,2}(\Omega_0) : \psi \text{ satisfies (2) and (3)}\}. \end{aligned} \quad (11)$$

Let  $H_0$  denote the self-adjoint operator associated with  $Q_D^{\Omega_0}$  via the first representation theorem [9, Thm. VI.2.1]. We claim that  $H_0 = -\Delta_D^{\Omega_0}$ . Indeed, by an integration by parts, it is easy to see that  $-\Delta_D^{\Omega_0} \subset H_0$ . The opposite inclusion  $-\Delta_D^{\Omega_0} \supset H_0$  can be checked with help of standard elliptic regularity theory (cf. [5, Sec. 3] for an analogous problem). Finally, the resolvent of  $-\Delta_D^{\Omega_0}$  is compact as a consequence of the compactness of the Sobolev embedding  $W^{2,2}(\Omega_0) \hookrightarrow L^2(\Omega_0)$ .  $\square$

In order to determine the spectrum of  $-\Delta_D^{\Omega_0}$ , it is convenient to consider the extended strip

$$\tilde{\Omega}_0 := (-2\pi R, 2\pi R) \times (-a, a)$$

and the associated Laplacian  $T_0$  in  $L^2(\tilde{\Omega}_0)$  with combined Dirichlet and standard periodic boundary conditions,

$$\begin{aligned} T_0 \psi &:= -\Delta \psi, \\ \mathsf{D}(T_0) &:= \left\{ \psi \in W^{2,2}(\tilde{\Omega}_0) : \psi \text{ satisfies } \begin{aligned} &\psi(s, \pm a) = 0, \quad \forall s \in (-2\pi R, 2\pi R), \\ &\text{and } \psi(-2\pi R, t) = \psi(2\pi R, t), \quad \partial_1 \psi(-2\pi R, t) = \partial_1 \psi(2\pi R, t), \quad \forall t \in (-a, a) \end{aligned} \right\}. \end{aligned}$$

This operator is well known to be self-adjoint and its spectrum can be easily found by separation of variables:

$$\sigma(T_0) = \left\{ \left( \frac{m}{2R} \right)^2 + \left( \frac{n\pi}{2a} \right)^2 \right\}_{\substack{m \in \mathbb{Z} \\ n \in \mathbb{N}^*}}.$$

The corresponding normalised eigenfunctions of  $T_0$  read

$$\phi_{m,n}(s, t) = \varphi_m(s) \chi_n(t)$$

with

$$\varphi_m(s) := \sqrt{\frac{1}{4\pi R}} e^{i \frac{m}{2R} s}, \quad \chi_n(t) := \begin{cases} \sqrt{\frac{1}{a}} \cos\left(\frac{n\pi}{2a} t\right) & \text{if } n \text{ is odd,} \\ \sqrt{\frac{1}{a}} \sin\left(\frac{n\pi}{2a} t\right) & \text{if } n \text{ is even.} \end{cases} \quad (12)$$

As eigenfunctions of a self-adjoint operator, it is also well known that  $\{\phi_{m,n}\}_{m \in \mathbb{Z}, n \in \mathbb{N}^*}$  is a complete orthonormal set in  $L^2((-2\pi R, 2\pi R) \times (-a, a))$ .

By symmetry properties of  $\varphi_m$  and  $\chi_n$ , we have

$$\begin{aligned} \phi_{m,n}(2\pi R, -t) &= (-1)^{m+n+1} \phi_{m,n}(0, t), \\ \partial_1 \phi_{m,n}(2\pi R, -t) &= (-1)^{m+n+1} \partial_1 \phi_{m,n}(0, t). \end{aligned}$$

Therefore we see that  $\phi_{m,n}$  satisfies the boundary conditions (3)–(4) if, and only if,  $m+n$  is odd. Consequently,

$$\sigma(-\Delta_D^{\Omega_0}) \supset \left\{ \left( \frac{m}{2R} \right)^2 + \left( \frac{n\pi}{2a} \right)^2 \right\}_{\substack{m \in \mathbb{Z} \\ n \in \mathbb{N}^* \\ m+n \text{ odd}}} \quad (13)$$

and the corresponding normalised eigenfunctions of  $-\Delta_D^{\Omega_0}$  are given by the restrictions

$$\psi_{m,n} := \sqrt{2} \phi_{m,n} \upharpoonright \Omega_0, \quad m \in \mathbb{Z}, \quad n \in \mathbb{N}^*, \quad m+n \text{ is odd.} \quad (14)$$

To show that the right-hand side of (13) determines *all* the eigenvalues of  $-\Delta_D^{\Omega_0}$ , we need the following result.

**Proposition 2.**  $\{\psi_{m,n}\}_{m \in \mathbb{Z}, n \in \mathbb{N}^*, m+n \text{ odd}}$  is a complete orthonormal set in  $L^2(\Omega_0)$ .

*Proof.* The property that  $\{\phi_{m,n}\}_{m \in \mathbb{Z}, n \in \mathbb{N}^*}$  is a complete orthonormal set in  $L^2(\tilde{\Omega}_0)$  is equivalent to the validity of the Parseval equality

$$\|f\|^2 = \sum_{m \in \mathbb{Z}, n \in \mathbb{N}^*} |(\phi_{m,n}, f)|^2 \quad (15)$$

for every  $f \in L^2(\tilde{\Omega}_0)$ , where  $\|\cdot\|$  and  $(\cdot, \cdot)$  denote the norm and inner product of  $L^2(\tilde{\Omega}_0)$ , respectively. Given an arbitrary  $g \in L^2(\Omega_0)$ , we define the extension

$$f(s, t) := \begin{cases} g(s, t) & \text{if } s > 0, \\ g(s + 2\pi R, -t) & \text{if } s < 0. \end{cases} \quad (16)$$

By an obvious integral substitution, it is straightforward to check the identity

$$\|f\|^2 = 2 \|g\|^2, \quad (17)$$

where on the right-hand side we use the same notation  $\|\cdot\|$  for the norm of  $L^2(\Omega_0)$ . At the same time, using in addition to the substitution the symmetry properties of  $\varphi_m$  and  $\chi_n$ , we have

$$(\phi_{m,n}, f) = \frac{1}{\sqrt{2}} [1 + (-1)^{m+n+1}] (\psi_{m,n}, g), \quad (18)$$

where on the right-hand side we use the same notation  $(\cdot, \cdot)$  for the inner product of  $L^2(\Omega_0)$ . Putting (17) and (18) into (15), we get the Parseval equality

$$\|g\|^2 = \sum_{\substack{m \in \mathbb{Z}, n \in \mathbb{N}^* \\ m+n \text{ odd}}} |(\psi_{m,n}, g)|^2,$$

which is equivalent to the desired completeness result.  $\square$

As a consequence of this proposition and (13), we conclude with the desired result (5). The elements of the set (5) will be denoted by  $\lambda_{m,n}$ .

**Remark 1.** The lowest eigenvalue

$$\lambda_{0,1} = E_1$$

is simple and the corresponding eigenfunction  $\psi_{0,1}$  is positive. In particular, the inequality (10) is optimal. The eigenvalues  $\lambda_{m,n}$  with  $m \neq 0$  are always degenerate. In particular, the second eigenvalue

$$\min\{\lambda_{1,2} = \lambda_{-1,2}, \lambda_{2,1} = \lambda_{-2,1}\}$$

is always degenerate. Furthermore, if  $\pi R = a$  then the second eigenvalue has multiplicity four.

### 3 The not-so-fake model

Since  $V_{\text{eff}}$  is real-valued and bounded, the operator sum  $H_{\text{eff}} := -\Delta_D^{\Omega_0} + V_{\text{eff}}$  in (6) defines a self-adjoint operator. As in the fake model, together with  $H_{\text{eff}}$  in  $L^2(\Omega_0)$ , we also consider  $T_{\text{eff}} := T_0 + V_{\text{eff}}$  in the extended Hilbert space  $L^2(\tilde{\Omega}_0)$ . The eigenvalues and eigenfunctions of  $T_{\text{eff}}$  can be found by separation of variables. In the second variable we get the same result as in the previous section: the normalised eigenfunctions of the Laplacian in  $L^2((-a, a))$ , subject to Dirichlet boundary conditions, are numbered by  $n \in \mathbb{N}^*$  and given by  $\chi_n$  as in (12) and the corresponding eigenvalues are  $E_1 n^2$ . The case of the

first variable is a little bit more involved. After the separation of variables, we arrive at the differential equation

$$-\varphi''(s) - \frac{1}{8R^2} \cos\left(\frac{s}{R}\right) \varphi(s) = \nu\varphi(s). \quad (19)$$

It turns out that this is the Mathieu differential equation. Before we proceed any further let us first review basic properties of Mathieu functions.

**Remark 2** (Mathieu functions). We use the following notation (see [1, §28.2]). Fix  $q, \mu \in \mathbb{R}$  and consider the ordinary differential equation

$$y''(\eta) + (\mu - 2q \cos(2\eta))y(\eta) = 0. \quad (20)$$

This equation has a  $2\pi$ -periodic solution if, and only if,  $\mu = a_m(q)$  or  $\mu = b_m(q)$ , where  $a_m(q)$  with  $m \in \mathbb{N}$  and  $b_m(q)$  with  $m \in \mathbb{N}^*$  are the so-called Mathieu characteristic values. These characteristic values satisfy

$$\begin{aligned} q > 0: & \quad a_0 < b_1 < a_1 < b_2 < a_2 < \dots, \\ q < 0: & \quad a_0 < a_1 < b_1 < b_2 < a_2 < \dots, \\ q = 0: & \quad a_m(0) = b_m(0) = m^2. \end{aligned} \quad (21)$$

The Mathieu integral order functions  $ce_m(\eta, q)$  with  $m \in \mathbb{N}$  and  $se_m(\eta, q)$  with  $m \in \mathbb{N}^*$  are defined in the following way:  $ce_m(\eta, q)$  is the even solution of (20) with  $\mu = a_m(q)$  and  $se_m(\eta, q)$  is the odd solution of (20) with  $\mu = b_m(q)$ . Both  $ce_m(\cdot, q)$  and  $se_m(\cdot, q)$  are  $2\pi$ -periodic. Moreover,  $ce_{2m}(\cdot, q)$  and  $se_{2m+2}(\cdot, q)$  are  $\pi$ -periodic and  $ce_{2m+1}(\cdot, q)$  and  $se_{2m+1}(\cdot, q)$  are antiperiodic with antiperiod  $\pi$ . For any  $q \in \mathbb{R}$ , the integral order Mathieu functions  $ce_m(\eta, q)$  and  $se_m(\eta, q)$  taken together form an orthogonal basis in  $L^2((-\pi, \pi))$  (see [2, §20.5]). We assume both  $ce_m(\eta, q)$  and  $se_m(\eta, q)$  are normalised to  $\sqrt{\pi}$  in  $L^2((-\pi, \pi))$ , *i.e.* the equalities

$$\int_{-\pi}^{\pi} |ce_m(\eta, q)|^2 d\eta = \int_{-\pi}^{\pi} |se_m(\eta, q)|^2 d\eta = \pi \quad (22)$$

hold for all possible values of  $m$ . This convention is in agreement with [1] and it is respected by Wolfram Mathematica, too. The (anti)periodicity then implies

$$\int_0^{\pi} |ce_m(\eta, q)|^2 d\eta = \int_0^{\pi} |se_m(\eta, q)|^2 d\eta = \frac{\pi}{2}. \quad (23)$$

Let us now return to the equation (19). Employing a simple change of the independent variable,  $\eta = s/(2R)$ , we immediately get the Mathieu equation (20) with  $q = -1/4$  and  $\mu = 4R^2\nu$ . Thus the equation (19) has the following  $(4\pi R)$ -periodic and normalised solutions if and only if  $\nu$  satisfies one of the indicated conditions

$$\varphi_m^{(1)}(s) := \frac{1}{\sqrt{\pi}} se_m\left(\frac{s}{2R}, -\frac{1}{4}\right) \quad \text{if } b_m\left(-\frac{1}{4}\right) = 4R^2\nu \quad \text{for some } m \in \mathbb{N}^*, \quad (24)$$

$$\varphi_m^{(2)}(s) := \frac{1}{\sqrt{\pi}} ce_m\left(\frac{s}{2R}, -\frac{1}{4}\right) \quad \text{if } a_m\left(-\frac{1}{4}\right) = 4R^2\nu \quad \text{for some } m \in \mathbb{N}. \quad (25)$$

The eigenvalues of  $T_{\text{eff}}$  therefore read

$$\sigma(T_{\text{eff}}) = \left\{ \left(\frac{1}{2R}\right)^2 a_m\left(-\frac{1}{4}\right) + \left(\frac{n\pi}{2a}\right)^2 \right\}_{\substack{m \in \mathbb{N} \\ n \in \mathbb{N}^*}} \cup \left\{ \left(\frac{1}{2R}\right)^2 b_m\left(-\frac{1}{4}\right) + \left(\frac{n\pi}{2a}\right)^2 \right\}_{\substack{m \in \mathbb{N}^* \\ n \in \mathbb{N}^*}}.$$

The corresponding normalised eigenfunctions are given by

$$\begin{aligned} \phi_{m,n}^{(1)}(s, t) &:= \varphi_m^{(1)}(s) \chi_n(t), & m \in \mathbb{N}^*, n \in \mathbb{N}^*, \\ \phi_{m,n}^{(2)}(s, t) &:= \varphi_m^{(2)}(s) \chi_n(t), & m \in \mathbb{N}, n \in \mathbb{N}^*, \end{aligned}$$

and they form a complete orthonormal set of  $L^2(\tilde{\Omega}_0)$ .

Let us now find the eigenfunctions and eigenvalues of the not-so-fake Möbius-strip operator  $H_{\text{eff}}$ . Note that for any  $j = 1, 2$  the functions  $\varphi_m^{(j)}$  are antiperiodic (respectively, periodic) with antiperiod  $2\pi R$  (respectively, period  $2\pi R$ ) whenever  $m$  is odd (respectively, even). Using this observation we establish the following symmetry properties of the eigenfunctions of  $T_{\text{eff}}$ :

$$\phi_{m,n}^{(j)}(s + 2\pi R, -t) = \varphi_m^{(j)}(s + 2\pi R)\chi_n(-t) = (-1)^m \varphi_m^{(j)}(s)(-1)^{n+1}\chi_n(t) = (-1)^{m+n+1} \phi_{m,n}^{(j)}(s, t), \quad (26)$$

for any  $j = 1, 2$  and all permissible  $m$  and  $n$ . In particular, setting  $s = 0$  in the last equation we have

$$\phi_{m,n}^{(j)}(2\pi R, -t) = (-1)^{m+n+1} \phi_{m,n}^{(j)}(0, t)$$

and so  $\phi_{r,n}^{(j)}$  with  $j = 1, 2$  satisfies the boundary conditions (3)–(4) if, and only if,  $m + n$  is odd. Consequently,

$$\sigma(H_{\text{eff}}) \supset \left\{ \left( \frac{1}{2R} \right)^2 a_m \left( -\frac{1}{4} \right) + \left( \frac{n\pi}{2a} \right)^2 \right\}_{\substack{m \in \mathbb{N} \\ n \in \mathbb{N}^* \\ m+n \text{ odd}}} \cup \left\{ \left( \frac{1}{2R} \right)^2 b_m \left( -\frac{1}{4} \right) + \left( \frac{n\pi}{2a} \right)^2 \right\}_{\substack{m \in \mathbb{N}^* \\ n \in \mathbb{N} \\ m+n \text{ odd}}}. \quad (27)$$

The corresponding normalised eigenfunctions of  $H_{\text{eff}}$  are given by the restrictions

$$\psi_{m,n}^{(j)} := \sqrt{2} \phi_{m,n}^{(j)} \upharpoonright \Omega_0,$$

where  $(m, n) \in \mathbb{N}^* \times \mathbb{N}^* =: \mathbb{N}_1$  if  $j = 1$  and  $(m, n) \in \mathbb{N} \times \mathbb{N}^* =: \mathbb{N}_2$  if  $j = 2$ . That the normalisation factor  $\sqrt{2}$  is correct follows from the final equations (22) and (23) in Remark 2 and equations (24)–(25).

To show that the right-hand side of (27) determines *all* the eigenvalues of  $H_{\text{eff}}$ , we need the following result analogous to Proposition 2.

**Proposition 3.**  $\{\psi_{m,n}^{(j)}\}_{j=1,2, (m,n) \in \mathbb{N}_j, m+n \text{ odd}}$  is a complete orthonormal set in  $L^2(\Omega_0)$ .

*Proof.* The property that the set  $\{\phi_{m,n}^{(j)}\}_{j=1,2, (m,n) \in \mathbb{N}_j}$  is a complete orthonormal set in  $L^2(\tilde{\Omega}_0)$  is equivalent to the validity of the Parseval equality

$$\|f\|^2 = \sum_{\substack{(m,n) \in \mathbb{N}_j \\ j=1,2}} |(\phi_{m,n}^{(j)}, f)|^2 \quad (28)$$

for every  $f \in L^2(\tilde{\Omega}_0)$ . Given an arbitrary  $g \in L^2(\Omega_0)$ , we define the extension  $f \in L^2(\tilde{\Omega}_0)$  as in (16). By an obvious integral substitution, it is straightforward to check the identity (17). At the same time, using in addition to the substitution the symmetry property (26), we have

$$\begin{aligned} (\phi_{m,n}^{(j)}, f) &= \int_{(-2\pi R, 0) \times (-a, a)} \phi_{m,n}^{(j)}(s, t) g(s + 2\pi R, -t) \, ds \, dt + \int_{(0, 2\pi R) \times (-a, a)} \phi_{m,n}^{(j)}(s, t) g(s, t) \, ds \, dt \\ &= \int_{(0, 2\pi R) \times (-a, a)} \phi_{m,n}^{(j)}(s - 2\pi R, -t) g(s, t) \, ds \, dt + \frac{1}{\sqrt{2}} \int_{(0, 2\pi R) \times (-a, a)} \psi_{r,n}^{(j)}(s, t) g(s, t) \, ds \, dt \\ &= \frac{(-1)^{m+n+1}}{\sqrt{2}} \int_{(0, 2\pi R) \times (-a, a)} \psi_{m,n}^{(j)}(s, t) g(s, t) \, ds \, dt + \frac{1}{\sqrt{2}} \int_{(0, 2\pi R) \times (-a, a)} \psi_{m,n}^{(j)}(s, t) g(s, t) \, ds \, dt \\ &= \frac{1}{\sqrt{2}} [(-1)^{m+n+1} + 1] (\psi_{m,n}^{(j)}, g). \end{aligned} \quad (29)$$

Putting (17) and (29) into (28), we get the Parseval inequality

$$\|g\|^2 = \sum_{\substack{(m,n) \in \mathbb{N}_j \\ j=1,2 \\ m+n \text{ odd}}} |(\psi_{m,n}^{(j)}, g)|^2,$$

which is equivalent to the desired completeness result.  $\square$

As a consequence of this proposition and (27), we conclude with the desired result (8). Note that the particular Mathieu characteristic values  $a_m(-1/4)$  and  $b_m(-1/4)$  appearing in (8) do not depend on  $a$  neither  $R$ . However, their value gets very close to each other with increasing  $m$ . First few of these values are presented in Table 1. Consequently, the not-so-fake model exhibits pairs of eigenvalues located very close each other (also recall (21)).

$m$	$a_m$	$b_m$
0	-0.03103939547561732443850972818046737540	
1	0.74242882598662974339949054767095543815	1.24194112824291514482231057477841662622
2	4.02582908464560324171350493521402514557	3.99479307863211894594328093443536761399
3	9.00366486704623913463365662695182921571	9.00415255154693478030510107620470513307
4	16.00208529046719562998287970766353836899	16.00208190103817298727073812993351765300
5	25.00130213222684081366209108945453834337	25.00130214546980228095721811268235655121
6	36.00089287379843422726407677439950789279	36.00089287376532391463296827349981967276
7	49.00065104784806396399969278784780613747	49.00065104784812144953869393158610105146
8	64.00049603440671169350384368118283820869	64.00049603440671162017886328541877470187
9	81.00039062627570760760462351056102476286	81.00039062627570760767623083270127588410
10	100.00031565723007867410511381290959992431	100.00031565723007867410505855991940003139

Table 1: Mathieu characteristic values  $a_m(-1/4)$  and  $b_m(-1/4)$  occurring in the spectrum (8) of the not-so-fake model computed by Wolfram Mathematica.

## 4 From the true to the not-so-fake model

By definition (1),  $\Omega = \mathcal{L}([0, 2\pi R) \times (-a, a))$ , where  $\mathcal{L} : \mathbb{R}^2 \rightarrow \mathbb{R}^3$  is given by

$$\mathcal{L}(s, t) := \left( \left[ R - t \cos\left(\frac{s}{2R}\right) \right] \cos\left(\frac{s}{R}\right), \left[ R - t \cos\left(\frac{s}{2R}\right) \right] \sin\left(\frac{s}{R}\right), -t \sin\left(\frac{s}{2R}\right) \right).$$

Except for the segment  $\mathcal{L}(\{0\} \times (-a, a))$ , which has the Lebesgue measure equal to zero, it is thus possible to identify  $\Omega$  with the Riemannian manifold  $(\Omega_0, G)$ , where  $G := \nabla \mathcal{L} \cdot (\nabla \mathcal{L})^T$  is the metric induced by  $\mathcal{L}$ . It is straightforward to check that  $G$  has the diagonal form

$$G = \begin{pmatrix} f^2 & 0 \\ 0 & 1 \end{pmatrix} \quad \text{with} \quad f(s, t) := \sqrt{\left[ 1 - \frac{t}{R} \cos\left(\frac{s}{2R}\right) \right]^2 + \left(\frac{t}{2R}\right)^2}.$$

Without any restriction on the positive parameters  $a$  and  $R$ , the Jacobian  $f$  is always positive, and therefore  $(\Omega_0, G)$  is an immersed manifold. In fact, we have the uniform bounds

$$\frac{1}{5} \leq f(s, t)^2 \leq \left(1 + \frac{a}{R}\right)^2 + \left(\frac{a}{2R}\right)^2 \quad (30)$$

valid for every  $(s, t) \in \Omega_0$ . If one wants to make  $(\Omega_0, G)$  embedded (and keep the geometric interpretation via a non-overlapping Möbius strip  $\Omega$ ), it is needed to impose the condition  $a < R$ . For our purposes, however, it is enough to work in the more general, immersed setting.

In view of the identification above, the Laplace–Beltrami operator  $-\Delta_D^\Omega$  in  $L^2(\Omega)$  can be identified with the operator

$$H = -|G|^{-1/2} \partial_i |G|^{1/2} G^{ij} \partial_j \quad \text{in} \quad L^2(\Omega_0, |G(s, t)|^{1/2} ds dt),$$

subject to Dirichlet boundary conditions (2) and twisted periodic boundary conditions (3)–(4). Here we use the Einstein summation convention with the range of indices  $i, j = 1, 2$ ,  $|G(s, t)| := \det(G) = f^2$  and  $G^{ij}$  denote the coefficients of the inverse metric  $G^{-1}$ . More specifically,  $H$  is introduced as the self-adjoint operator associated with the closed quadratic form

$$h[\psi] := \int_{\Omega_0} \overline{\partial_i \psi(s, t)} G^{ij}(s, t) \partial_j \psi(s, t) |G(s, t)|^{1/2} ds dt, \\ \mathsf{D}(h) := \{ \psi \in W^{1,2}(\Omega_0) : \psi \text{ satisfies (2) and (3)} \}.$$

Notice that the form domain coincides with the form domain of the fake Möbius strip  $-\Delta_D^{\Omega_0}$  (cf. (11)) as well as the not-so-fake model  $H_{\text{eff}}$ .

Since we are interested in the limit  $a \rightarrow 0$ , it is convenient to introduce the unitary transform  $U : L^2(\Omega_0, f(s, t) ds dt) \rightarrow L^2(\Pi)$  by setting

$$(U\psi)(s, u) := \sqrt{a} \sqrt{f(s, au)} \psi(s, au),$$

where  $\Pi$  is the  $a$ -independent rectangle

$$\Pi := (0, 2\pi R) \times (-1, 1). \quad (31)$$

Define the unitarily equivalent operator  $L := UHU^{-1}$  in  $L^2(\Pi)$ , which is the operator associated with the quadratic form  $l[\phi] := h[U^{-1}\phi]$ ,  $D(l) := UD(h)$ .

**Proposition 4.** *One has*

$$l[\phi] = \int_{\Pi} \frac{|\partial_1 \phi(s, u)|^2}{f_a(s, u)^2} ds du + \frac{1}{a^2} \int_{\Pi} |\partial_2 \phi(s, u)|^2 ds du + \int_{\Pi} V_a(s, u) |\phi(s, u)|^2 ds du,$$

$$D(l) = \left\{ \phi \in W^{1,2}(\Pi) : \phi(s, \pm 1) = 0 \text{ for } s \in (0, 2\pi R) \text{ and } \phi(0, u) = \phi(2\pi R, -u) \text{ for } u \in (-1, 1) \right\},$$

where  $f_a(s, u) := f(s, au)$  and

$$V_a := -\frac{5}{4} \frac{(\partial_1 f_a)^2}{f_a^4} + \frac{1}{2} \frac{\partial_1^2 f_a}{f_a^3} - \frac{1}{4} \frac{(\partial_2 f_a)^2}{a^2 f_a^2} + \frac{1}{2} \frac{\partial_2^2 f_a}{a^2 f_a}.$$

*Proof.* The mapping property  $UW^{1,2}(\Omega_0) = W^{1,2}(\Pi)$  is easily checked with help of (30) and the fact that there is a constant  $C$  such that  $|\nabla f(s, t)| \leq C$  for every  $(s, t) \in \Omega_0$ . If  $\psi$  satisfies the Dirichlet boundary conditions (2), then  $\phi := U\psi$  clearly satisfies  $\phi(s, \pm 1) = 0$  for almost every  $s \in (0, 2\pi R)$ . At the same time, if  $\psi$  satisfies the twisted periodic boundary condition (3), then  $\phi$  satisfies  $\phi(0, u) = \phi(2\pi R, -u)$  for almost every  $u \in (-1, 1)$  due to the symmetry property  $f(2\pi R, au) = f(0, -au)$ . These prove the identity for the form domain  $D(l)$ .

Now, let  $\psi \in D(h)$  and  $\phi := U\psi$ . Then, making the change of variables and integrating by parts, we have

$$\begin{aligned} h[\psi] &= \int_{\Pi} \overline{\partial_i \phi} G_a^{ij} \partial_j \phi - \int_{\Pi} \frac{1}{2} \frac{\partial_i f_a}{f_a} G_a^{ij} \partial_j |\phi|^2 + \int_{\Pi} \frac{1}{4} \frac{\partial_i f_a}{f_a} G_a^{ij} \frac{\partial_i f_a}{f_a} |\phi|^2 \\ &= \int_{\Pi} \overline{\partial_i \phi} G_a^{ij} \partial_j \phi + \int_{\Pi} \left[ \frac{1}{2} \partial_j \left( \frac{\partial_i f_a}{f_a} G_a^{ij} \right) + \frac{1}{4} \frac{\partial_i f_a}{f_a} G_a^{ij} \frac{\partial_i f_a}{f_a} \right] |\phi|^2, \end{aligned}$$

where  $G_a(s, u) := \text{diag}(f_a^2, a^2)$  and the arguments  $(s, u) \in \Pi$  of the functions and the measure of integration  $ds du$  are suppressed. Here it is crucial that the boundary terms due to the integration by parts vanish. This is easy to see when we integrate by parts with respect to the second variable, because of the Dirichlet boundary conditions  $\phi(s, \pm 1) = 0$  for almost every  $s \in (0, 2\pi R)$ . To see it also when we integrate by parts with respect to the first variable, we notice the property  $\partial_1 f_a(0, u) = 0 = \partial_1 f_a(2\pi R, u)$  for every  $u \in (-1, 1)$ . Using the special form of  $G_a$ , we get the desired formula.  $\square$

We observe that there exists an  $a$ -independent constant  $C$  such that

$$|f_a(s, u) - 1| \leq Ca \quad (32)$$

and

$$\begin{aligned} |\partial_1 f_a(s, u)| &\leq Ca, & |\partial_1^2 f_a(s, u)| &\leq Ca^2, \\ \left| \frac{\partial_2 f_a(s, u)}{a} + \frac{1}{R} \cos\left(\frac{s}{2R}\right) \right| &\leq Ca, & \left| \frac{\partial_2^2 f_a(s, u)}{a^2} - \frac{1}{(2R)^2} \right| &\leq Ca, \end{aligned}$$

for every  $(s, u) \in \Pi$ . Hereafter we use the convention that  $C$  denotes an  $a$ -independent constant which may change its value from one line to another. Consequently, there exists another constant  $C$  such that

$$|V_a(s, u) - V_{\text{eff}}(s, au)| \leq Ca \quad (33)$$

for every  $(s, u) \in \Pi$ , where  $V_{\text{eff}}$  is defined in (6).

**Remark 3.** Since  $\Omega$  is a ruled surface, the straight lines  $t \mapsto \mathcal{L}(s, t)$  are geodesics for every fixed  $s \in [0, 2\pi R)$ . Consequently,  $(s, t)$  are Fermi coordinates and we have the simple formula

$$K := -\frac{\partial_2^2 f}{f}$$

for the Gauss curvature of  $\Omega$ . At the same time, using the normal vector field  $\partial_2 \mathcal{L}$  (actually independent of the second variable) along the unit-speed circle  $s \mapsto \mathcal{L}(s, 0)$  as a curve on  $\Omega$ , we have the formula

$$\kappa_g(s) = \partial_1 \mathcal{L}(s, 0) \cdot \partial_2 \mathcal{L}(s, 0) = \frac{1}{R} \cos\left(\frac{s}{2R}\right)$$

for the geodesic curvature of the circle. Consequently,

$$V_{\text{eff}}(s, t) = -\frac{1}{4}\kappa_g(s)^2 - \frac{1}{2}K(s, 0),$$

in agreement with the case of general thin strips [10, Sec. 3]. Notice that while the geodesic curvature has a jump at the endpoints of the Möbius strip, namely  $\kappa_g(0) = -\kappa_g(2\pi R)$ , which reflects the fact that  $\Omega$  is not orientable, the effective potential  $V_{\text{eff}}$  extends to a *smooth* function on  $\Omega$ .

In order to compare the true Möbius strip  $H$  (which is unitarily equivalent to  $L$  in  $L^2(\Pi)$ ) with the not-so-fake model  $H_{\text{eff}}$  in  $L^2(\Omega_0)$ , we also map the latter to an operator in the  $a$ -independent Hilbert space  $L^2(\Pi)$ . This is achieved by the unitary transform  $U_{\text{eff}} : L^2(\Omega_0) \rightarrow L^2(\Pi)$  that acts as

$$(U_{\text{eff}}\psi)(s, u) := \sqrt{a}\psi(s, au).$$

It is elementary to check that the unitarily equivalent operator  $L_{\text{eff}} := U_{\text{eff}}H_{\text{eff}}(U_{\text{eff}})^{-1}$  is associated with the quadratic form

$$\begin{aligned} l_{\text{eff}}[\phi] &:= \int_{\Pi} |\partial_1 \phi(s, u)|^2 ds du + \frac{1}{a^2} \int_{\Pi} |\partial_2 \phi(s, u)|^2 ds du + \int_{\Pi} V_{\text{eff}}(s, au) |\phi(s, u)|^2 ds du, \\ \mathbf{D}(l_{\text{eff}}) &:= \mathbf{D}(l), \end{aligned}$$

where  $\mathbf{D}(l)$  is given in Proposition 4.

Now we are in a position to establish the norm-resolvent convergence.

**Theorem 1.** *For every  $z \notin \sigma(L - E_1) \cup \sigma(L_{\text{eff}} - E_1)$ , there exists an  $a$ -independent constant  $C$  such that, for all positive  $a$ ,*

$$\|(L - E_1 - z)^{-1} - (L_{\text{eff}} - E_1 - z)^{-1}\| \leq Ca, \quad (34)$$

where  $\|\cdot\|$  denotes the operator norm in  $L^2(\Pi)$ .

*Proof.* Using (9) and an elementary estimate of  $V_{\text{eff}}$ , we have

$$L_{\text{eff}} - E_1 \geq -\frac{1}{8R^2}.$$

Consequently, any negative  $z$  with sufficiently large  $|z|$  (with the largeness independent of  $a$ ) belongs to the resolvent set of  $H_{\text{eff}}$ . Using (33), the same conclusion holds for  $L$ . Fixing such an  $a$ -independent  $z$  and given arbitrary functions  $f, g \in L^2(\Pi)$ , let us consider the resolvent equations

$$(L_{\text{eff}} - E_1 - z)\phi = f \quad \text{and} \quad (L - E_1 - z)\psi = g. \quad (35)$$

The first equation implies

$$l_{\text{eff}}[\phi] - E_1 \|\phi\|^2 - z \|\phi\|^2 = (\phi, f) \leq \|\phi\| \|f\|,$$

where  $\|\cdot\|$  and  $(\cdot, \cdot)$  denote the norm and inner product of  $L^2(\Pi)$ . Recalling (9), we obtain

$$\|\phi\| \leq C \|f\| \quad \text{and} \quad \|\partial_1 \phi\|^2 \leq C \|f\|^2, \quad (36)$$

where  $C := [|z| - (8R^2)^{-1}]^{-1}$ . Similarly, using in addition (32) and (33), the second equation of (35) yields

$$\|\psi\| \leq C \|g\| \quad \text{and} \quad \|\partial_1 \psi\|^2 \leq C \|g\|^2 \quad (37)$$

with some  $a$ -independent constant  $C$ . Let us now write

$$\begin{aligned} (f, [(L - E_1 - z)^{-1} - (L_{\text{eff}} - E_1 - z)^{-1}]g) &= (f, (L - E_1 - z)^{-1}g) - ((L_{\text{eff}} - E_1 - z)^{-1}f, g) \\ &= ((L_{\text{eff}} - E_1 - z)\phi, \psi) - (\phi, (L - E_1 - z)\psi) \\ &= l_{\text{eff}}(\phi, \psi) - l(\phi, \psi), \end{aligned} \quad (38)$$

where  $l(\cdot, \cdot)$  (respectively,  $l_{\text{eff}}(\cdot, \cdot)$ ) denotes the sesquilinear form associated with  $l[\cdot]$  (respectively,  $l_{\text{eff}}[\cdot]$ ). The last identity employs the fact that the form domains of  $L$  and  $L_{\text{eff}}$  coincide. We have

$$\begin{aligned} |l(\phi, \psi) - l_{\text{eff}}(\phi, \psi)| &= |(\partial_1 \phi, [f_a^{-2} - 1] \partial_1 \psi) + (\phi, [V_a - V_{\text{eff}}] \psi)| \\ &\leq Ca \|\partial_1 \phi\| \|\partial_1 \psi\| + Ca \|\phi\| \|\psi\| \\ &\leq Ca \|f\| \|g\|, \end{aligned} \tag{39}$$

where the first estimate follows by (32) and (33) together with the Schwarz inequality and the second inequality employs (36) and (37). Combining (38) and (39), we obtain (34). In view of [9, Rem. IV.3.13], the estimate (34) extends to any  $z$  in the resolvent sets of  $L$  and  $L_{\text{eff}}$ .  $\square$

As a particular consequence of (34) and [8, Chapter II, Corrolary 2.3], we get the convergence of eigenvalues of  $L$  to the eigenvalues of  $L_{\text{eff}}$ . More specifically, for fixed real  $z \notin \sigma(L) \cup \sigma(L_{\text{eff}})$  and every  $j \in \mathbb{N}^*$ , we have

$$\left| \frac{1}{\lambda_j(L) - E_1 - z} - \frac{1}{\lambda_j(L_{\text{eff}}) - E_1 - z} \right| \leq Ca,$$

where the  $a$ -independent constant  $C$  is the same as in (34) and  $\{\lambda_j(A)\}_{j \in \mathbb{N}^*}$  denotes the non-decreasing sequence of eigenvalues of a self-adjoint operator  $A$  with compact resolvent, where each eigenvalue is repeated according to its multiplicity (*cf.* [7, Sec. 4.5]). The eigenvalues  $\lambda_j(L_{\text{eff}})$  are known explicitly, see (8). In particular, given any  $j \in \mathbb{N}^*$ , the shifted eigenvalue  $\lambda_j(L_{\text{eff}}) - E_1$  is independent of  $a$  for all sufficiently small  $a$  (with the smallness depending on  $j$ ) and we thus get the following result.

**Corollary 1.** *For every  $k \in \mathbb{N}^*$ , there exist positive  $a$ -independent constants  $C_k$  and  $a_k$  such that, for all  $a \leq a_k$ ,*

$$\forall j \in \{1, \dots, k\}, \quad |\lambda_j(L) - \lambda_j(L_{\text{eff}})| \leq C_k a.$$

The convergence in norm of corresponding spectral projections also follows.

## 5 Numerical results

In this closing section, we will numerically investigate properties of the eigenvalues and eigenfunctions of the true and not-so-fake Möbius models described above. In view of the unitary equivalence described in Section 4, our starting point is the operator  $L$  associated with the quadratic form  $l$  introduced in Proposition 4. It corresponds to the operator

$$L = -\partial_1 \frac{1}{f_a^2} \partial_1 - \frac{1}{a^2} \partial_2^2 + V_a \quad \text{in} \quad L^2(\Pi),$$

subject to Dirichlet boundary conditions

$$\psi(s, \pm 1) = 0 \tag{40}$$

for almost every  $s \in (0, 2\pi R)$  and twisted periodic boundary conditions

$$\psi(0, u) = \psi(2\pi R, -u), \tag{41}$$

$$\partial_1 \psi(0, u) = \partial_1 \psi(2\pi R, -u), \tag{42}$$

for almost every  $u \in (-1, 1)$ . The rectangular domain is defined in (31) and the functions  $V_a$  and  $f_a$  can be found in Proposition 4.

In order to numerically analyse solutions of the eigenvalue problem  $Lf = \lambda f$ , we employ a particular orthonormal basis of  $L^2(\Pi)$  formed by eigenfunctions of the fake model,

$$\mathcal{B} := \{\Psi_{m,n}\}_{\substack{m \in \mathbb{Z}, n \in \mathbb{N}^* \\ m+n \text{ is odd}}} \subset L^2(\Pi),$$

where  $\Psi_{m,n}(s, u) := \sqrt{a} \psi_{m,n}(s, au)$  and  $\psi_{m,n}$  is defined in (14). For convenience, let us arrange the eigenvalues (5) of the fake model in a non-decreasing sequence  $\{\lambda_j^{(\text{fake})}\}_{j \in \mathbb{N}^*}$ , where each eigenvalue

is repeated according to its multiplicity. The set of corresponding eigenfunctions will be denoted by  $\mathcal{B} = \{\Psi_j\}_{j \in \mathbb{N}^*}$ . Thus

$$\left(-\partial_1^2 - \frac{1}{a^2}\partial_2^2\right)\Psi_j = \lambda_j^{(\text{fake})}\Psi_j$$

and  $\Psi_j$  with  $j \in \mathbb{N}^*$  obey the Dirichlet (40) as well as twisted periodic boundary conditions (41)–(42).

Now let us fix a large  $N \in \mathbb{N}^*$  and consider the orthogonal projection  $P_N$  onto the linear span of the truncated orthonormal set  $\mathcal{B}_N = \{\Psi_j\}_{j=1}^N$ . Instead of the full eigenvalue problem for  $L$  we solve the finite-dimensional eigenvalue problem for  $P_N L P_N$ . In other words, we compute eigenvalues and eigenvectors of the matrix  $M \in \mathbb{R}^{N,N}$  with entries

$$M_{jk} = (\Psi_j, L\Psi_k), \quad j, k = 1, \dots, N,$$

where  $(\cdot, \cdot)$  denotes the inner product in  $L^2(\Pi)$ . The resulting eigenvalues  $\tilde{\lambda}_1^{(\text{true})} \leq \tilde{\lambda}_2^{(\text{true})} \leq \dots \leq \tilde{\lambda}_N^{(\text{true})}$  are upper estimates (cf. [7, Sec. 4.5]) of the true Möbius eigenvalues, *i.e.* we have  $\lambda_j^{(\text{true})} \leq \tilde{\lambda}_j^{(\text{true})}$ ,  $j = 1, 2, \dots, N$ . Corresponding approximations to the true eigenvectors are then

$$\tilde{f}_k = \sum_{j=1}^N c_j^{(k)} \Psi_j,$$

where  $c^{(k)} = (c_1^{(k)}, \dots, c_N^{(k)})^T$  is an eigenvector of  $M$  with eigenvalue  $\tilde{\lambda}_k^{(\text{true})}$ . Note that the entries of  $M$  have to be evaluated numerically, in particular we have the following expression

$$\begin{aligned} \langle \Psi_{m,n}, L\Psi_{k,\ell} \rangle &= \frac{mk}{4R^2} \int_{\Pi} \frac{1}{f_a(s,u)^2} \Psi_{-m,n}(s,u) \Psi_{-k,\ell}(s,u) \, ds \, du + \frac{1}{a^2} \left(\frac{n\pi}{2}\right)^2 \delta_{mk} \delta_{n\ell} + \\ &+ \int_{\Pi} V_a(s,u) \Psi_{m,n}(s,u) \Psi_{k,\ell}(s,u) \, ds \, du, \end{aligned}$$

where  $\delta_{mn}$  is the usual Kronecker symbol.

**Remark 4.** Before we conclude this section with the presentation of our numerical results, let us make two remarks. The matrix  $M$  is a  $N \times N$  real symmetric and full matrix (*i.e.* not a sparse one). Its eigenvalues and eigenvectors can be computed numerically using one's favorite computer algebra system, we use the Julia programming environment [4]. All of our code is available in a public GitHub repository<sup>1</sup>. The reason for taking the eigenvectors of the fake model instead of not-so-fake model is that it is much easier to work with sines and cosines instead of Mathieu functions.

Let us conclude this section with a short review of the results of our numerical experiments. In Figure 2 one can see the eigenfunctions of the operator  $L$  with  $a = 1.3$  and  $R = 18/(2\pi)$ . It is also interesting to visualize eigenvectors as living on the original Möbius strip. This is the purpose of Figure 3 where we have taken  $a = 0.75$  and  $R = 13.2/(2\pi)$ . Table 2 contains approximations of the corresponding first twenty eigenvalues of the operator  $L$ .

Finally, we wish to test the expected asymptotic behavior of the not-so-fake and true model as the thickness of the Möbius strip  $a$  goes to zero (recall Theorem 1). Let  $\lambda_n^{(\text{not-so-fake})}(a)$  and  $\lambda_n^{(\text{true})}(a)$  denote the  $n$ th eigenvalue of the operator  $L_{\text{eff}}$  and  $L$ , respectively. The former is known explicitly (see equation (8)), the latter can be computed numerically as described in the previous paragraphs. The resulting approximation will be denoted by  $\tilde{\lambda}_n^{(\text{true})}$ .

In order to test the convergence rate we plot the ratio

$$\frac{|\lambda_n^{(\text{not-so-fake})} - \tilde{\lambda}_n^{(\text{true})}|}{a^2}$$

for  $n = 1, \dots, 20$  and  $a$  ranging from 0.01 to 1.5 with  $R = 18/(2\pi)$ , see Figure 4. In this particular case we also check convergence of the corresponding normalized eigenvectors. In Figure 5 we plot the ratio

$$\frac{\|\tilde{f}_n - f_n^{(\text{not-so-fake})}\|_{L^2(\Pi)}}{a^2}.$$

Both of these experiments suggest that the convergence rate is quadratic as  $a$  goes to 0 and so the Corollary 1 is only a good upper estimate.

<sup>1</sup><https://github.com/kalvotom/moebius>

## Acknowledgment

The research of D.K. was partially supported by the GACR grant No. 18-08835S. The research of T.K. was supported by the Ministry of Education, Youth and Sports of the Czech Republic project no. CZ.02.1.01/0.0/0.0/16\_019/0000778.

## References

- [1] *NIST digital library of mathematical functions*, <http://dlmf.nist.gov/>, Release 1.0.15 of 2017-06-01 (F. W. J. Olver, A. B. Olde Daalhuis, D. W. Lozier, B. I. Schneider, R. F. Boisvert, C. W. Clark, B. R. Miller, and B. V. Saunders, eds.).
- [2] M. S. Abramowitz and I. A. Stegun, eds., *Handbook of mathematical functions*, Dover, New York, 1965.
- [3] R. A. Adams and J. J. F. Fournier, *Sobolev spaces*, Academic Press, 2003, 2nd edition.
- [4] J. Bezanson, A. Edelman, S. Karpinski, and V. B. Shah, *Julia: A Fresh Approach to Numerical Computing*, SIAM Review **59** (2017), 65-98, doi: 10.1137/141000671, url: <https://julialang.org/research/julia-fresh-approach-BEKS.pdf>.
- [5] D. Borisov and D. Krejčířík,  *$\mathcal{PJ}$ -symmetric waveguides*, Integ. Equ. Oper. Theory **62** (2008), 489–515.
- [6] J. H. E. Cartwright and D. L. González, *Möbius strips before Möbius: Topological hints in ancient representations*, Math. Intell. **38** (2016), 69–76.
- [7] E. B. Davies, *Spectral theory and differential operators*, Cambridge University Press, Cambridge, 1995.
- [8] I. C. Gohberg and M. G. Krein, *Introduction to the theory of linear nonselfadjoint operators in Hilbert space*, American Mathematical Society, 1969.
- [9] T. Kato, *Perturbation theory for linear operators*, Springer-Verlag, Berlin, 1966.
- [10] D. Krejčířík, *Quantum strips on surfaces*, J. Geom. Phys. **45** (2003), no. 1–2, 203–217.
- [11] D. Krejčířík, N. Raymond, and M. Tušek, *The magnetic Laplacian in shrinking tubular neighbourhoods of hypersurfaces*, J. Geom. Anal. **25** (2015), 2546–2564.
- [12] Z. Li, L. R. Ram-Mohan, *Quantum mechanics on a Möbius ring: Energy levels, symmetry, optical transitions, and level splitting in a magnetic field*, Phys. Rev. B **85** (2012), 195438–195446.
- [13] C. B. Macdonald, J. Brandman, and S. J. Ruuth, *Solving eigenvalue problems on curved surfaces using the closest point method*, J. Comput. Phys. **230** (2011), 7944–7956.
- [14] C. A. Pickover, *The Möbius strip: Dr. August Möbius’s marvelous band in mathematics, games, literature, art, technology, and cosmology*, Basic Books, 2007.

$n$	$\tilde{\lambda}_n^{(\text{true})}$	$\ L\tilde{f}_n - \tilde{\lambda}_n^{(\text{true})}\tilde{f}_n\ _{L^2(\Pi)}$	$\lambda_n^{(\text{not-so-fake})}$	$\lambda_n^{(\text{fake})}$
1	4.387440201465426	0.0011360336639659758	4.384732657634105	4.386490844928603
2	4.619975308169118	0.002935713704540701	4.612770845791257	4.613065785265825
3	4.6210487512326965	0.0034765508104058836	4.61452884109396	4.613065785265825
4	5.311812674844678	0.009392208389967776	5.292908532928366	5.292790606277488
5	5.311812691949888	0.009394620959796087	5.292908724918286	5.292790606277488
6	6.45928381512197	0.01784426849679324	6.425715883668621	6.425665307963595
7	6.459283815177474	0.017844019253709244	6.425715883670497	6.425665307963595
8	8.054793717112888	0.02782741553208048	8.011717987565671	8.011689890324144
9	8.054793717134626	0.02782929178936725	8.011717987565671	8.011689890324144
10	10.087710686170643	0.07623428743234176	10.050882233363655	10.050864353359135
11	10.087710686180136	0.07623425520146826	10.050882233363655	10.050864353359135
12	12.544971054834159	0.12299616532523619	12.543201075519463	12.543188697068569
13	12.544971054880232	0.12299618315689324	12.543201075519463	12.543188697068569
14	15.411764278613166	0.15141422162634224	15.48867199897889	15.488662921452445
15	15.411764278618152	0.1514142253244023	15.48867199897889	15.488662921452445
16	17.59842628782262	0.005712405600055002	17.58801732145255	17.602607114798715
17	17.622050913758347	0.003779453318856355	17.616311563972907	17.602607114798715
18	18.084500866091076	0.017503712257836673	18.055964587231244	18.05575699547316
19	18.084502386722757	0.01752620443224552	18.055992211502907	18.05575699547316
20	18.672740544194298	0.18297451968432338	18.887293968147098	18.88728702651077

Table 2: First twenty approximations of the eigenvalues of the true model  $\tilde{\lambda}_n^{(\text{true})}$  and norms of residues  $L\tilde{f}_n - \tilde{\lambda}_n^{(\text{true})}\tilde{f}_n$ , where  $\tilde{f}_n$  is the normalised eigenvector of  $M$  corresponding to  $\tilde{\lambda}_n^{(\text{true})}$ . Value of parameters are  $a = 0.75$ ,  $R = 13.2/(2\pi)$ , and  $N = 82$ . For convenience we also present eigenvalues of the not-so-fake  $\lambda_n^{(\text{not-so-fake})}$  and fake model  $\lambda_n^{(\text{fake})}$ , see (8) and (5), respectively.

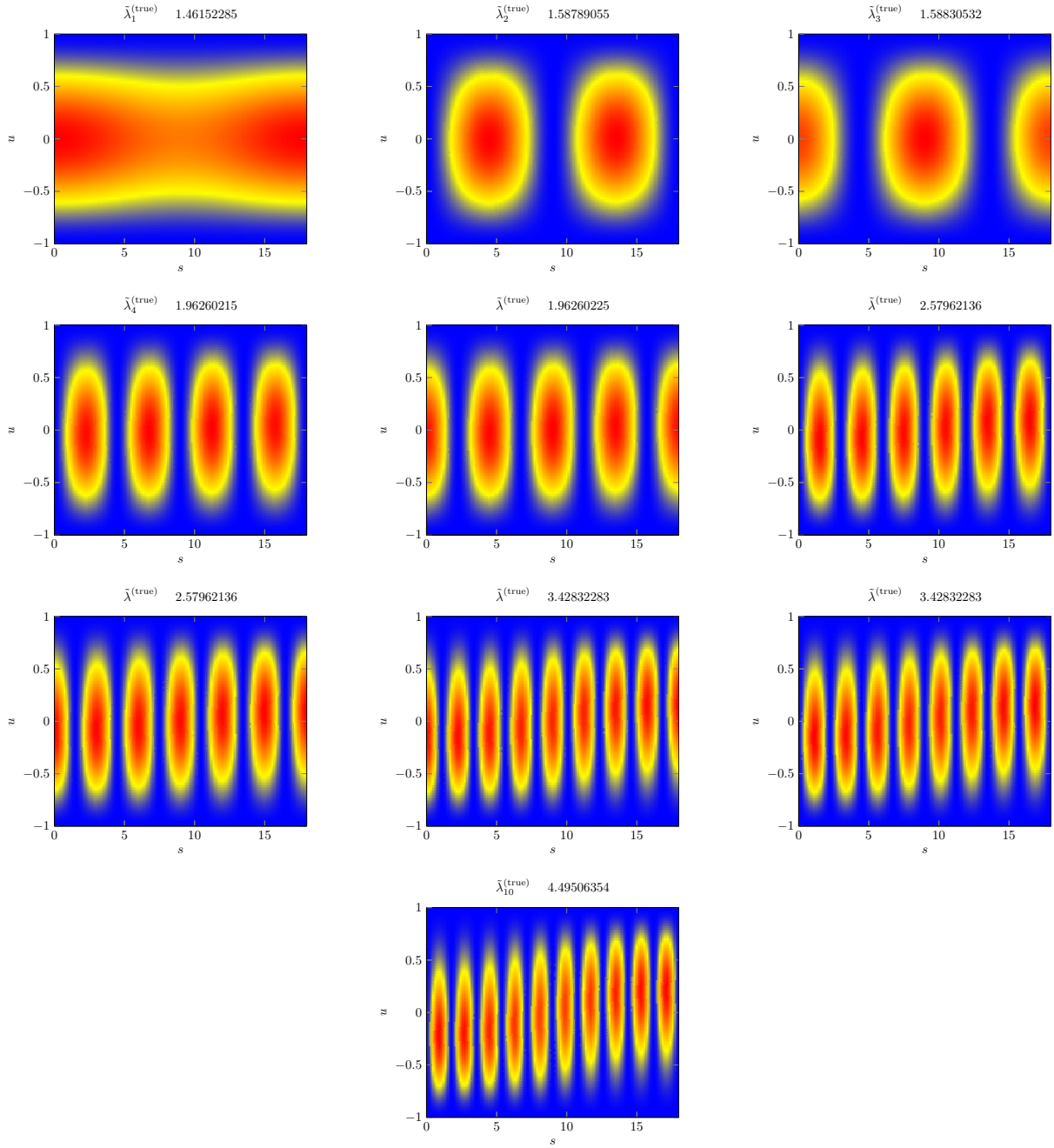


Figure 2(a): Numerical approximations  $\tilde{f}_k$  of eigenvalues and eigenfunctions of the operator  $L$  for  $k = 1, 2, \dots, 10$ . We are plotting probability densities  $|f_k|^2$ , blue and red color corresponds to zero and maximal value, respectively. Parameters of the numerical computation are  $a = 1.3$ ,  $R = 18/(2\pi)$ , and  $N = 96$ .

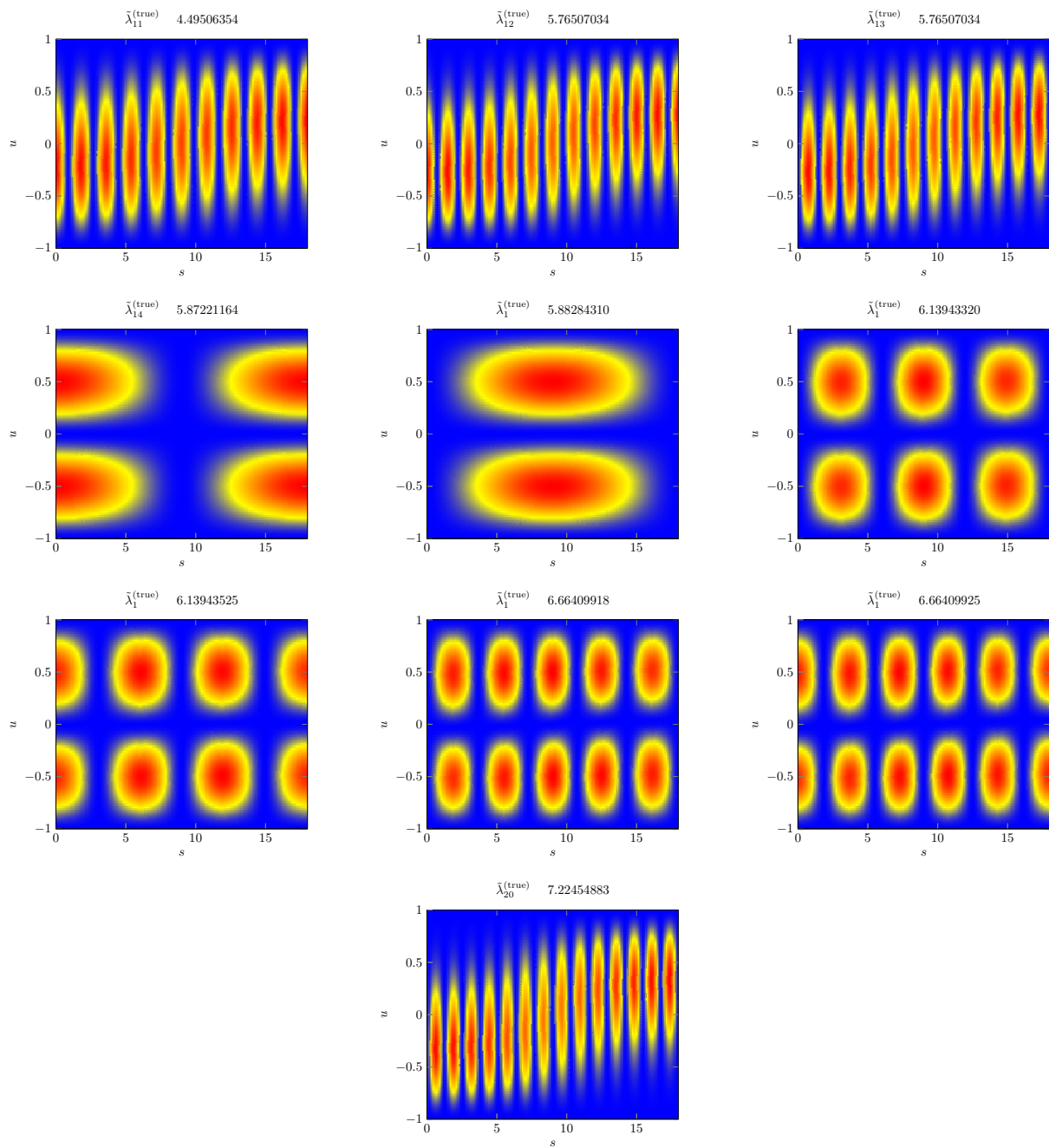


Figure 2(b): Numerical approximations  $\tilde{f}_k$  of eigenvalues and eigenfunctions of the operator  $L$  for  $k = 11, 12, \dots, 20$ . We are plotting probability densities  $|\tilde{f}_k|^2$ , blue and red color corresponds to zero and maximal value, respectively. Parameters of the numerical computation are  $a = 1.3$ ,  $R = 18/(2\pi)$ , and  $N = 96$ .

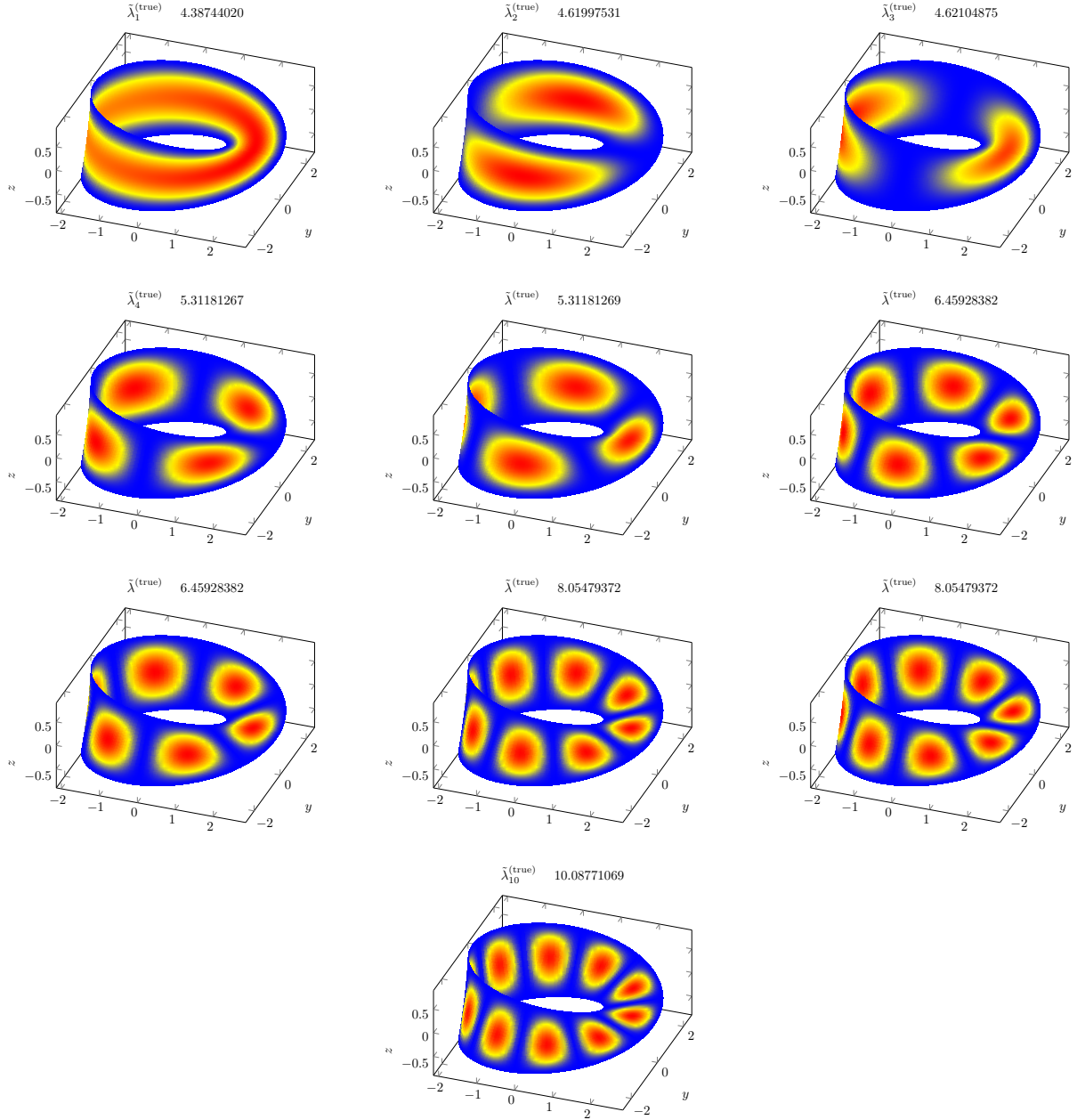


Figure 3(a): Numerical approximations  $\tilde{f}_k$  of eigenvalues and eigenfunctions of the operator  $L$  for  $k = 1, 2, \dots, 10$  plotted onto the original Möbius strip. Parameters of the numerical computation are  $a = 0.75$ ,  $R = 13.2/(2\pi)$ , and  $N = 82$ . Color coding is the same as in Figure 2.

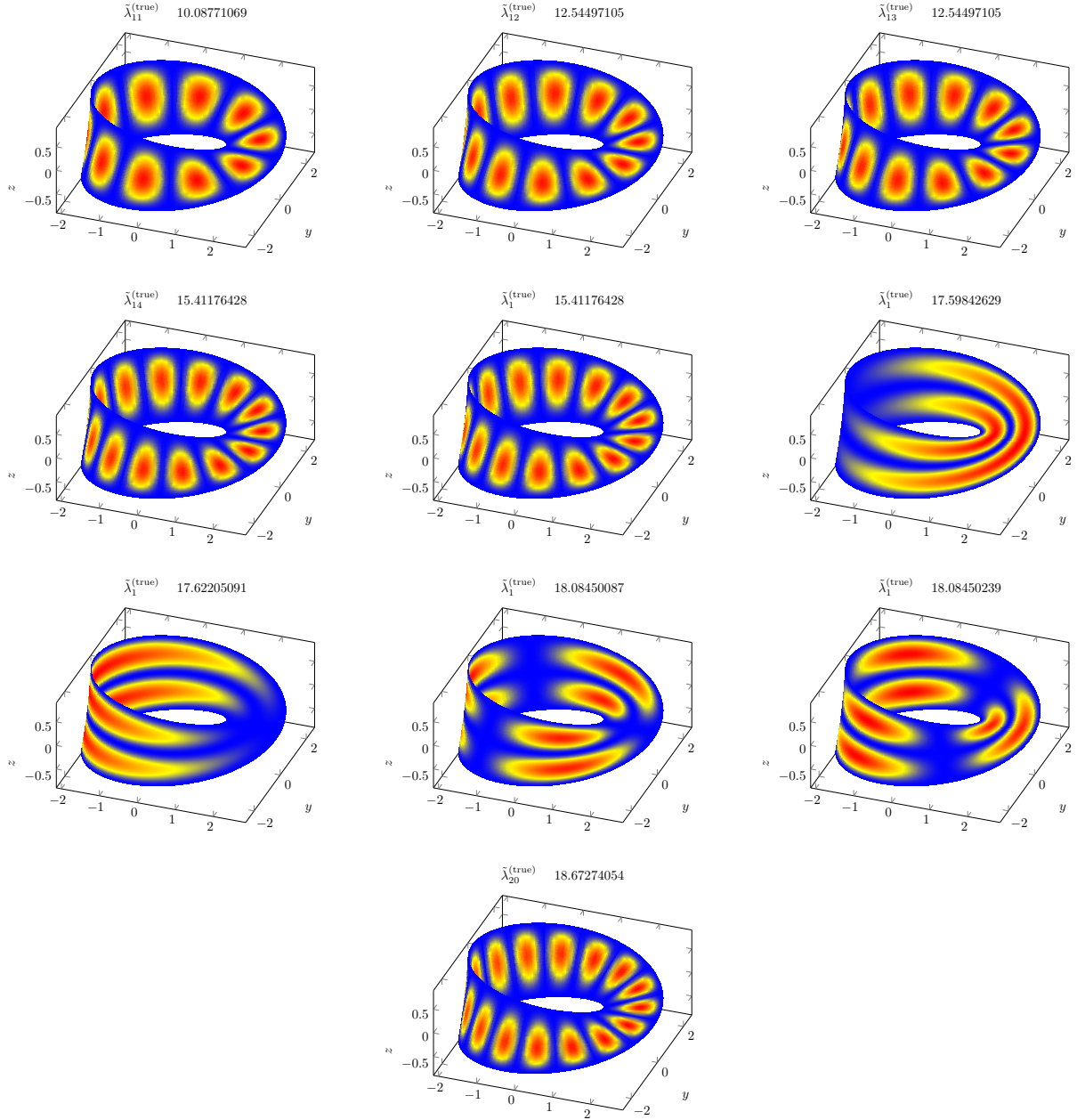


Figure 3(b): Numerical approximations  $\tilde{f}_k$  of eigenvalues and eigenfunctions of the operator  $L$  for  $k = 11, 12, \dots, 20$  plotted onto the original Mbius strip. Parameters of the numerical computation are  $a = 0.75$ ,  $R = 13.2/(2\pi)$ , and  $N = 82$ . Color coding is the same as in Figure 2.

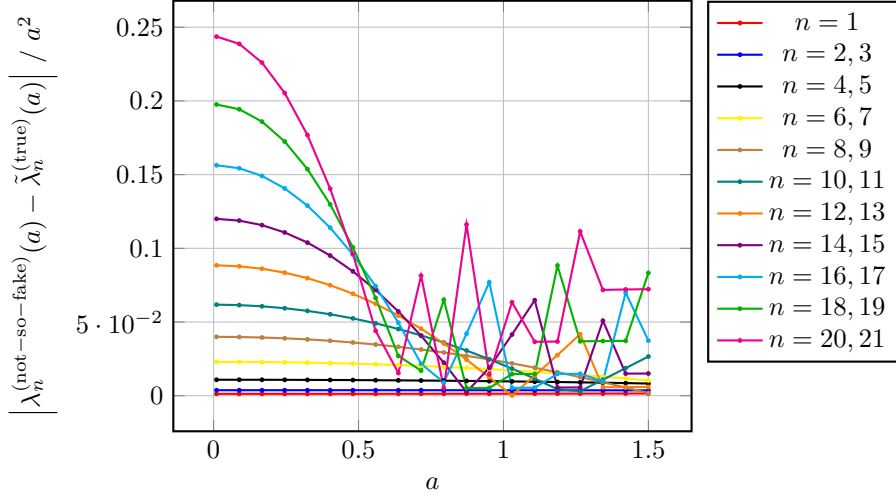


Figure 4: Ratio of the difference of the  $n$ th eigenvalue of the not-so-fake model  $\lambda_n^{(\text{not-so-fake})}(a)$  and numerical approximation of the  $n$ th eigenvalue of the full model  $\tilde{\lambda}_n^{(\text{full})}(a)$  and  $a^2$ ,  $n = 1, \dots, 20$ . Values of parameters are  $R = 18/(2\pi)$ ,  $a$  ranges from 0.01 to 1.5, and  $N = 72$ . Each curve, except the one for  $n = 1$ , in fact represents two of these ratios which are indistinguishable in this plot resolution.

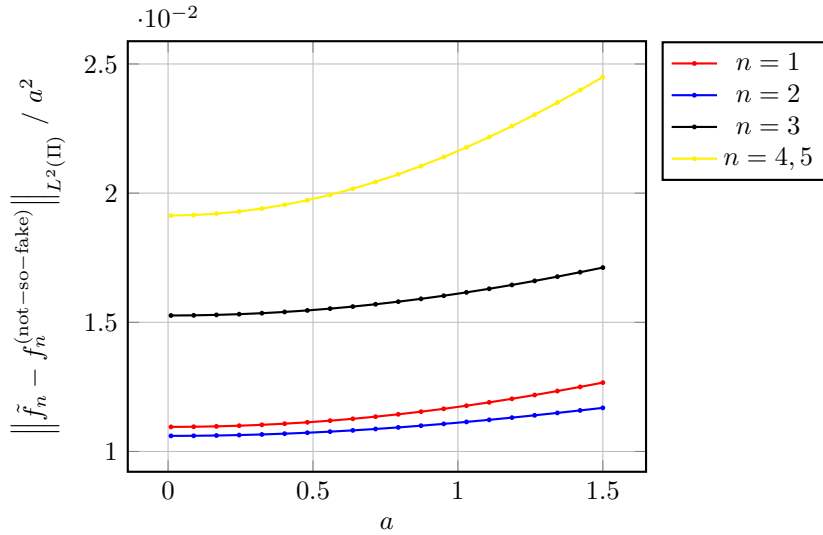


Figure 5: Ratio of the norm of the difference of the  $n$ th eigenvector of the not-so-fake model  $f_n^{(\text{not-so-fake})}$  and numerical approximation of the  $n$ th eigenvector of the full model  $\tilde{f}_n$  and  $a^2$ ,  $n = 1, \dots, 5$ . Values of parameters are  $R = 18/(2\pi)$ ,  $a$  ranges from 0.01 to 1.5, and  $N = 72$ .